Formaldehyde Emission Behavior of Building Materials: On-Site Measurements and Modeling Approach to Predict Indoor Air Pollution

D. Bourdin, Pierre Mocho, V. Desauziers, H. Plaisance

Formaldehyde emission behavior of building materials: On-site measurements and modeling approach to predict indoor air pollution

Delphine Bourdin[a,b], Pierre Mocho[c,*], Valérie Desauziers[a], Hervé Plaisance[a]

[a] Pôle RIME C2MA, Ecole des Mines d'Alès, Hélioparc, 2 Avenue Pierre Angot, 64053 Pau Cedex 9, France
[b] NOBATEK, 67 Rue de Mirambeau, 64600 Anglet, France
[c] Laboratoire Thermique Energétique et Procédés, Université de Pau et des Pays de l'Adour, BP 7511, 64075 Pau, France

HIGHLIGHTS

- New method to measure gas phase concentration of formaldehyde at material surface.
- New method to quantify the mass transfer of formaldehyde at material surface.
- Assessment of a mass balance model to predict indoor air quality.
- On-site measurements were required to predict their real impact on indoor pollution.

ABSTRACT

The purpose of this paper was to investigate formaldehyde emission behavior of building materials from on-site measurements of air phase concentration at material surface used as input data of a box model to estimate the indoor air pollution of a newly built classroom. The relevance of this approach was explored using CFD modeling. In this box model, the contribution of building materials to indoor air pollution was estimated with two parameters: the convective mass transfer coefficient in the mate-rial/air boundary layer and the on-site measurements of gas phase concentration at material surfaces. An experimental method based on an emission test chamber was developed to quantify this convective mass transfer coefficient. The on-site measurement of gas phase concentration at material surface was measured by coupling a home-made sampler to SPME. First results had shown an accurate estimation of indoor formaldehyde concentration in this classroom by using a simple box model.

Keywords:
Formaldehyde
Indoor air quality
Building material
On-site emission cell
Box model
CFD modeling
SPME

1. Introduction

Exposure to indoor air pollutants was one of the primary environmental health stressors, since people spend 80–90% of their time within enclosed living spaces [1]. Among indoor pollutants, volatile organic compounds (VOCs) were of environmental interest because they could be responsible for health hazards and/or malodorous atmospheres [2]. Regarding the large number of indoor sources such as building materials, furniture, burning of petroleum products, smoking, electrical appliances, use of cleaning products and other household chemicals, they were found to be present at higher concentrations in indoor air than outdoors [3]. To limit their levels, one strategy consisted on control of their major emission sources, especially building materials [4,5]. In France, as in several European countries, new products were evaluated through a time-consuming procedure involving a 28-days emission test within an environmental chamber or an emission cell [6]. These

Abbreviations: A_j, external surface area of the material j (m^2); C_i, average indoor air concentration of the pollutant i ($\mu g\,m^{-3}$); C_{i0}, average indoor air concentration of pollutant i at $t=0$ ($\mu g\,m^{-3}$); C_{iout}, average outdoor air concentration of pollutant i ($\mu g\,m^{-3}$); C_{sij}, gas phase concentration of the pollutant i at material j surface ($\mu g\,m^{-3}$); D_{iair}, molecular diffusion of the pollutant i in the air ($m^2\,s^{-1}$); H, height of the room (m); h_{ij}, convective mass transfer coefficient of pollutant i through the boundary layer over the material j ($m\,s^{-1}$); i, pollutant (formaldehyde or carbon dioxyde); j, material number; L, length of the room (m); l, width of the room (m); L_c, characteristic length of the material/fluid system (m); m, total number of materials within the room; Q_{ij}, contribution of the material j to the IAQ (source or sink of pollutant i) ($\mu g\,m^{-3}\,s^{-1}$); t, time (s); t_{spme}, extraction time of the SPME fiber (min); U, mean air flow velocity over the material ($m\,s^{-1}$); U_m, mean air flow velocity inside the room ($m\,s^{-1}$); V, volume of the room (m^3); V_C, volume of the chamber test (50 L); ν, kinematic viscosity of the air ($m^2\,s^{-1}$); λ, outdoor air exchange rate (s^{-1}); λ_C, air exchange rate inside the chamber (s^{-1}); τ_{ij}, formaldehyde emission rate of the material j in the chamber test ($\mu g\,m^2\,s^{-1}$).

* Corresponding author. Tel.: +33 5 4017 5144; fax: +33 5 5940 7740.
E-mail address: pierre.mocho@univ-pau.fr (P. Mocho).

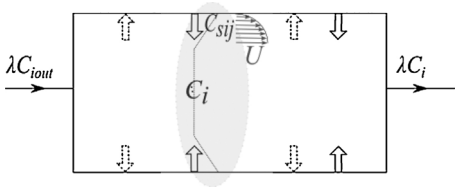

Fig. 1. Physical concept of the one-box model.

test methods were based on a dynamic sampling mode to transfer the VOCs emitted from the material to an active sampling tube to concentrate the compounds [7,8]. Thus, clean air supply, air flow meters and control of temperature and humidity were needed. These protocols, covered by ISO standards [9,10], were suitable for laboratory testing for material labeling but were not able to evaluate the material behavior in real indoor environments in the aim of determining their impact on indoor air quality. For this purpose, static sampling methods [11–14] have been recently investigated to obtain simpler and faster on-site sampling. One of these methods consisted of coupling a standard FLEC® emission cell in static mode with solid-phase microextraction (SPME) for rapid sampling and simple thermal desorption, directly performed in a GC injector and allowed a multi-pollutant analysis [15,16]. Assuming that equilibrium was reached inside the emission cell, the headspace concentration could be considered as the gas phase concentration at the material surface and quantified with a SPME fiber [17]. The ability to measure in situ the surface concentration of building materials offered opportunities to predict the indoor air quality (IAQ) and personal exposure level by modeling approaches. Two major types of computer simulation techniques for modeling IAQ were developed: mass-balance models and computational fluid dynamics (CFD) techniques [18]. Mass-balance models were used to simulate average indoor air pollutant concentration as a function of outdoor concentration, building characteristics (volume, air exchange rate...) and indoor sources/sinks. They were widely used due to the simplicity of the mathematics involved [19–21]. CFD models concerned a microscopic view of IAQ by examining the detailed flow fields and pollutant concentration distributions within a room. Some significant difficulties with CFD concerned the conception, the meshing of the geometry and the setup of the model. Moreover, calculation step was time consuming [22–24]. The developed model was inspired from box models, which were the oldest and most widely used to study the indoor environments [19]. A CFD model was also implemented to discuss the relevance of the box model in the studied indoor environment.

2. Theory/calculation

2.1. One-box model

The simple one-box model (or single zone model) described the change of a pollutant's indoor concentration in a well-mixed room as a differential equation, in which production processes add to the concentration with time and loss processes subtract from the concentration with time. Variants of the model relied on the definition of production and loss processes. Many studies had focused on the chemical reactivity of indoor pollutants, based on data from tropospheric chemistry [25–28] or on the sorption of VOCs on building materials [29]. In our approach, building materials were considered both as VOC sources and sinks from indoor air. If VOC concentration at material surface was higher than indoor air concentration then the material was considered as a VOC emission source (Fig. 1). Inversely, if surface concentration was lower than indoor air concentration then the material was a VOC sink. Therefore, the behavior of the building material was a function of the value of indoor air concentration, which depended itself on outdoor air exchange rate (defined by outdoor airflow to room volume ratio). The originality of this work was the quantification of real contribution of materials on IAQ by on-site measurements of both gas phase concentration at material surface and indoor air concentration. The mass balance for a controlled volume could be expressed by the following differential equation (Fig. 1):

$$\frac{\partial C_i}{\partial t} = \sum_{j=1}^{m} Q_{ij} + \lambda C_{iout} - \lambda C_i \tag{1}$$

where C_i was the average indoor air concentration of the pollutant i ($\mu g\,m^{-3}$), Q_{ij} the contribution of the material j to the IAQ (source or sink of pollutant i) ($\mu g\,m^{-3}\,s^{-1}$), λ the outdoor air exchange rate (s^{-1}), C_{iout} the average outdoor air concentration of pollutant i ($\mu g\,m^{-3}$), t the time and m the total number of materials within the room. In Fig. 1, C_{sij} was the gas phase concentration of the pollutant i at the material j surface.

At the material/air interface, VOC mass transfer could be expressed as:

$$Q_{ij} = h_{ij}\frac{A_j}{V}(C_{sij} - C_i) \tag{2}$$

where h_{ij} was the convective mass transfer coefficient of pollutant i through the boundary layer over the material j, A_j the surface area of the material j and V the volume of the room.

Substituting (2) into (1), we obtained:

$$\frac{\partial C_i}{\partial t} = \sum_{j=1}^{m} h_{ij}\frac{A_j}{V}C_{sij} + \lambda C_{iout} - \left(\sum_{j=1}^{m} h_{ij}\frac{A_j}{V} + \lambda\right) C_i \tag{3}$$

Assuming h_{ij}, C_{sij}, λ, A_j, V and C_{iout} were constant, Eq. (3) could be integrated analytically to give:

$$C_i(t) = \frac{\sum_{j=1}^{m} h_{ij}(A_j/V)C_{sij} + \lambda C_{iout}}{\sum_{j=1}^{m} h_{ij}(A_j/V) + \lambda}\left(1 - e^{-\left(\sum_{j=1}^{m} h_{ij}(A_j/V)+\lambda\right)t}\right) + C_{i0}e^{-\left(\sum_{j=1}^{m} h_{ij}(A_j/V)+\lambda\right)t} \tag{4}$$

where C_{i0} was the indoor air concentration of pollutant i at $t = 0$ (generally, $C_{i0} = C_{iout}$).

At steady state, Eq. (3) became:

$$C_i = \frac{\sum_{m}^{j=1} h_{ij}(A_j/V)C_{sij} + \lambda C_{iout}}{\sum_{m}^{j=1} h_{ij}(A_j/V) + \lambda} \tag{5}$$

The h_{ij} coefficient was determined by two ways: one based on empirical equations and the other on experimental protocol using a chamber test, as detailed on Material and Methods section.

2.2. Determination of the convective mass transfer coefficient from empirical equations (h_{ij})

In laminar flow over a flat surface, the convective mass transfer coefficient (h_{ij}) could be deduced from relationship among Sherwood number (Sh), Schmidt number (Sc) and Reynolds number (Re) according to the following equation [30]:

$$Sh = 0.664 Sc^{1/3} Re^{1/2} \tag{6}$$

where $Sh = h_{ij}L_c/D_{iair}$, $Sc = \nu/D_{iair}$, $Re = UL_c/\nu$, ν was the kinematic viscosity of the air ($m^2\,s^{-1}$), U the mean air flow velocity over the material ($m\,s^{-1}$), L_c the characteristic length of the material/fluid system (m) and D_{iair} the molecular diffusion coefficient of the compound i in the air ($m^2\,s^{-1}$). This coefficient could be estimated through two main methods: the Fuller, Schettler and Giddings (FSG) method and the Wilke and Lee (WL) method [31].

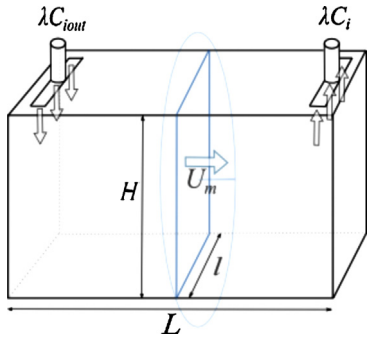

Fig. 2. Determination of the mean air velocity inside the room (U_m).

In addition, the calculation of h_{ij} required the knowledge of the mean air velocity over the material (U).

2.3. Determination of the mean air flow velocity over the material (U)

An accurate determination of this parameter close to the various materials of the room required the use of CFD models but this approach was quite difficult and time consuming. Nevertheless, a simplified approach could be considered according to the following method (Fig. 2). The room was considered as continuously stirred tank reactor (CSTR), operating at steady state conditions. The mean air flow velocity inside the room (U_m) could be then deduced from the following relationship:

$$V = HlU_m \tag{7}$$

where H and l were respectively the height and the width of the room (m), L the length of the room. It was assumed that the geometry of the room could be considered as a rectangular parallelepiped.

Here, the simplifying assumption consisted in considering the mean air flow velocity over the material (U) equal to the mean air flow velocity inside the room (U_m). So, the convective mass transfer coefficient of the pollutant i through the boundary layer (h_{ij}) had the same value for all materials present in the room.

Hence, Eq. (5) could be expressed as:

$$C_i = \frac{(h_{ij}/V)\sum_m^{j=1} A_j C_{sij} + \lambda C_{iout}}{(h_{ij}/V)\sum_m^{j=1} A_j + \lambda} \tag{8}$$

Eq. (8) was used to evaluate the VOC indoor air concentrations from the data of gas phase concentrations at material surfaces and airflow rate. The results were then compared to measured indoor air concentrations. Knowing the uncertainties of the used analytical devices ($\Delta h_{ij}/h_{ij} = 0.18$, $\Delta C_{sij}/C_{sij} = 0.16$, $\Delta\lambda/\lambda = 0.02$, $\Delta C_{iuot} = 2.3\ \mu g\,m^{-3}$), uncertainty of the predicted value was deduced from the following differential equation:

$$dC_i = \frac{\partial C_i}{\partial h_{ij}} dh_{ij} + \sum_{j=1}^{m} \frac{\partial C_i}{\partial C_{sij}} dC_{sij} + \frac{\partial C_i}{\partial \lambda} d\lambda + \frac{\partial C_i}{\partial C_{iout}} dC_{iout} \tag{9}$$

$$\text{with} \quad \frac{\partial C_i}{\partial h_{ij}} = \frac{(\sum_m^{j=1} A_j C_{sij}/V)\ (h_{ij}/V)\sum_m^{j=1} A_j + \lambda\ -(\sum_m^{j=1} A_j/V)\ (h_{ij}/V)\sum_m^{j=1} A_j C_{sij} + \lambda C_{iout}}{(h_{ij}/V)\sum_m^{j=1} A_j + \lambda\ ^2} \tag{10}$$

$$\frac{\partial C_i}{\partial C_{sij}} = \frac{(h_{ij}A_j/V)}{(h_{ij}/V)\sum_m^{j=1} A_j + \lambda}, \tag{11}$$

$$\frac{\partial C_i}{\partial C_{iout}} = \frac{\lambda}{(h_{ij}/V)\sum_m^{j=1} A_j + \lambda} \tag{12}$$

$$\frac{\partial C_i}{\partial \lambda} = \frac{C_{iout}\ (h_{ij}/V)\sum_m^{j=1} A_j + \lambda\ -\ (h_{ij}/V)\sum_m^{j=1} A_j C_{sij} + \lambda C_{iout}}{(h_{ij}/V)\sum_m^{j=1} A_j + \lambda\ ^2} \tag{13}$$

2.4. CFD modeling

ANSYS Fluent R15.0 software (Canonsburg, USA) was used to simulate fluid dynamics inside the experimental site. Based on Navier–Stockes equations, it solved both mass and momentum conservation equations using finite-volume method.

3. Materials and methods

3.1. Air sampling method

Air sampling was performed in 250 mL glass vial (Entech Instruments, Simi Valley, CA, USA) equipped with SPME-adapter (Quad Service, Achères, France) [32,33]. Vials were cleaned with humid nitrogen and evacuated before sampling thanks to a 3100A Canister Cleaner (Entech Instruments). On site, vials were filled with air by simply opening their vacuum valves and then stored no longer than two days at room temperature ($20 \pm 3\,^{\circ}C$). At laboratory, a preconditioned and modified SPME fiber was directly introduced in the vial through the SPME-adapter. The pre-concentration of formaldehyde was carried out for 30 min.

3.2. Material surface sampling method

A home-made cylindrical glass emission cell equipped with a septum for SPME fiber introduction was used in this study (Fig. 3). Its geometry was inspired by previous works [17].

The sampling involved two steps: first, the emission cell was directly placed on the material surface and formaldehyde was let to diffuse from the material to the headspace of the cell until reaching equilibrium (about two hours). This equilibrium time was deduced from material emission kinetics studies. Second, a pre-conditioned modified SPME fiber was introduced for 15 minutes for formaldehyde pre-concentration. This time is a good compromise between a correct analytical sensibility and a weak competitive adsorption of VOC. The fiber was then stored at room temperature ($20 \pm 3\,^{\circ}C$) in passivated stainless steel tubes no longer than 2 days before analysis [34].

3.3. SPME fiber modification

Formaldehyde was analyzed by on-fiber derivatization followed by gas chromatography. A poly(dimethylsiloxane)-divinylbenzene (PDMS-DVB) (65 μm) fiber (Supelco, Bellefonte, USA) was used. It was loaded with o-(2,3,4,5,6-pentafluorobenzyl)hydroxylamine hydrochloride (PFBHA) (Fluka, Brucks, Switzerland) [35].

3.4. Gas chromatography analysis

A 3800 gas chromatograph coupled with a 1200Q quadrupole mass spectrometer (GC–MS) (Varian, Les Ulis, France) was used for

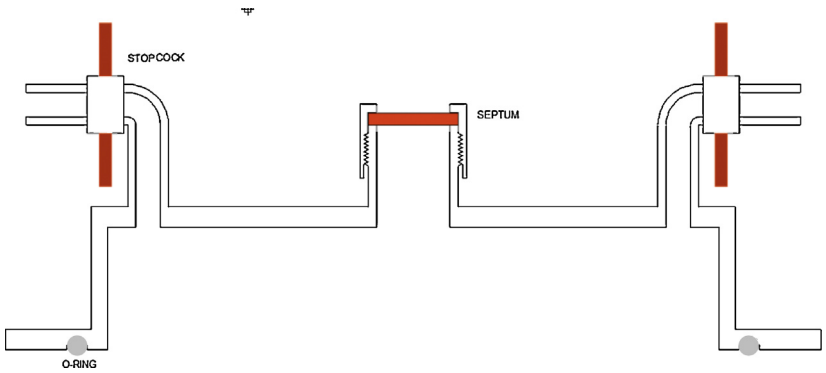

Fig. 3. Material surface sampling device.

quantification. It was equipped with a 60 m × 0.25 mm i.d. 1 μm Optima-5 Accent fused silica column (Macherey-Nagel, Düren, Deutschland). The PTV injection port was operated at 250 °C in splitless mode for SPME fiber desorption. Carrier gas was helium with a flow rate at 2 mL min^{-1}. The oven temperature was 40 °C (4-min hold) to 90 °C at 15 °C min^{-1} (4-min hold), then to 250 °C at 10 °C min^{-1} (5-min hold). Acquisition was carried out in single ion monitoring (SIM) mode. The m/z used for quantification was 181.

3.5. Standard gas generating device and calibration

Standard gas of formaldehyde was generated by a permeation device supplied by Calibrage (Saint Chamas, France). Detailed principle was described in previous papers [36,37]. Concentrations ranging from 1 to 400 μg m^{-3} were generated and calibration curves were plotted for both sampling devices: the 250 mL vial and the surface cylindrical glass sampler. SPME extraction and analysis were performed according to the method described above.

3.6. Air exchange rate measurement

Air exchange rate was determined from the depletion kinetic of injected CO_2 according to the standard method described in ASTM [38].

3.7. Determination of the experimental convective mass transfer coefficient h_{ij}

Two materials, known to be formaldehyde emitters, were studied: OSB (Oriented Strand Board) and MDF (Medium-density fiberboard). The OSB board was analyzed just after its purchase (OSB1) and after one month of storage in a ventilated room (OSB2). In order to determine the emission rate τ_{ij}, a material sample (20 cm × 20 cm) was introduced in a CLIMPAQ 50 L test chamber (Climtech, Copenhagen, Denmark) supplied with clean air at constant temperature (23 ± 2 °C) and relative humidity (50 ± 5% RH). The flow rate was ranged from 275 to 17,000 mL min^{-1} to study its influence on the emission rate. For each experiment, the formaldehyde concentration (C_i) in the chamber was determined after 2 days exposure according to the air sampling method described above. The gas phase concentration of formaldehyde at material surface (C_{sij}) was then determined by the surface sampling method (see Section 3.2)on the same material sample removed from the chamber and placed under the emission cell.

The formaldehyde emission rate of the material (τ_{ij}) was then calculated with the following equation:

$$\tau_{ij} = \frac{C_i \times V_C \times \lambda_C}{A_j} \quad (14)$$

where τ_{ij} was the formaldehyde emission rate of the material j (μg m^2 s^{-1}), C_i the formaldehyde concentration inside the CLIMAQ (μg m^{-3}), λ_C the air exchange rate inside the chamber (s^{-1}), V_C the volume of the test chamber (50 L) and A_j the j sample surface (m^2).

The convective mass transfer coefficient (h_{ij}) could be related to the formaldehyde emission rate of the material by the following equation:

$$\tau_{ij} = h_{ij}(C_{sij} - C_i) \quad (15)$$

As the chamber air concentration of formaldehyde (C_i) and the material surface concentration (C_{sij}) were known, the convective mass transfer coefficient (h_{ij}) of formaldehyde through the boundary layer over the material inside the chamber test could be deduced from Eq. (15).

3.8. On-site experiments

Main experiments for testing the model were carried out in a classroom of a new college, located in the South West of France (Table 1). The scheme of the classroom was shown in Fig. 4. The components of the room were detailed in Table 2. Student's desks were made of 19 mm-thick particle board. The chairs were made of beech wood recovered with a natural varnish. The ceiling was classified E1 according to the particle board French standard (NF EN 312). The door was also made of particle board and recovered

Table 1
Ventilation rate and dimensions of the studied classroom.

Classroom length L (m)	7.2
Width l (m)	6.9
Height H (m)	2.7
Air exchange rate λ (s^{-1})	9.17 × 10^{-4}

Table 2
Characteristics of components of the studied classroom.

Component (no.)	Material surface area A_j (m^2)
Whiteboard (1)	2.3
Interactive board (2)	1.9
Plastic flooring (3)	49.0
Suspended ceiling (4)	29.0
Chairs (5)	6.7
Upper side of desks (varnished particle board) (6)	10.0
Underside of desks (raw particle board) (7)	11.0
Painted walls (8)	52.2
Heater (9)	0.7
Polyester curtain (10)	11.0
Door (11)	2.0
Desk for disabled person (12)	1.0

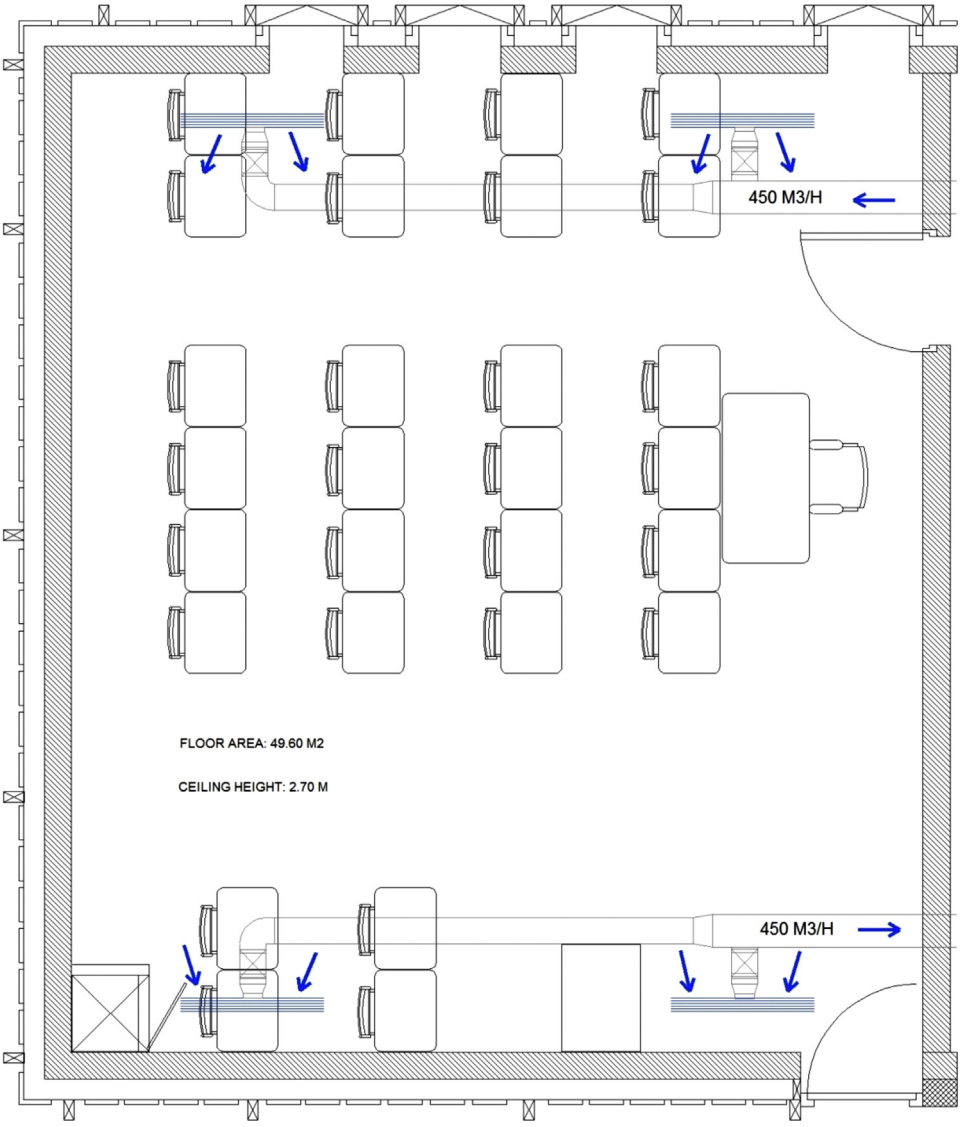

Fig. 4. Scheme of the studied classroom.

with MDF. Floor was covered with plastic coating and walls were painted. Five measurement campaigns were carried out over a period of 6 months. The first campaign (Week 1) was led just after the building delivery and the installation of the furniture.

3.9. CFD modeling

CFD modeling was applied to the experimental classroom with no furniture (Fig. 4). The simulation parameters were summarized in Table 3. Box model was also implemented to discuss its relevance.

4. Results and discussion

4.1. Characterization of the fluid flow inside the classroom

A simplifying assumption of the developed box model, consisted in considering the mean air flow velocity over the material (U) equal to the mean air flow velocity inside the room (U_m). To discuss the relevance of this point, a CFD simulation was carried out to characterize the air stream distribution in the studied room, according to the operating conditions presented in Table 3. Simulation results were presented in Fig. 5. As reference of flow velocity value, the

Table 3
CFD simulation main parameters.

Mesh	
Mesh method	Multizone
Mesh type	Hexahedral
Element size (m)	0.055
Inflation	
Boundary	6 faces (4 walls, floor, ceiling)
Inflation option	Total thickness
Number layers	5
Growth rate	1.2
Maximum thickness (m)	0.055
Nodes	1,230,953
Elements	1,199,536
Element size min–max (m^3)	3.34×10^{-6} to 3.71×10^{-4}
CFD fluent	
Model	Viscous–Realizable k-epsilon
Boundary conditions	
Inlet velocity ($m\,s^{-1}$)	
Inlet 1	0.463
Inlet 2	0.463
Formaldehyde mass fraction	
Inlet 1 and 2	4.08×10^{-9}
Floor	1.063×10^{-8}

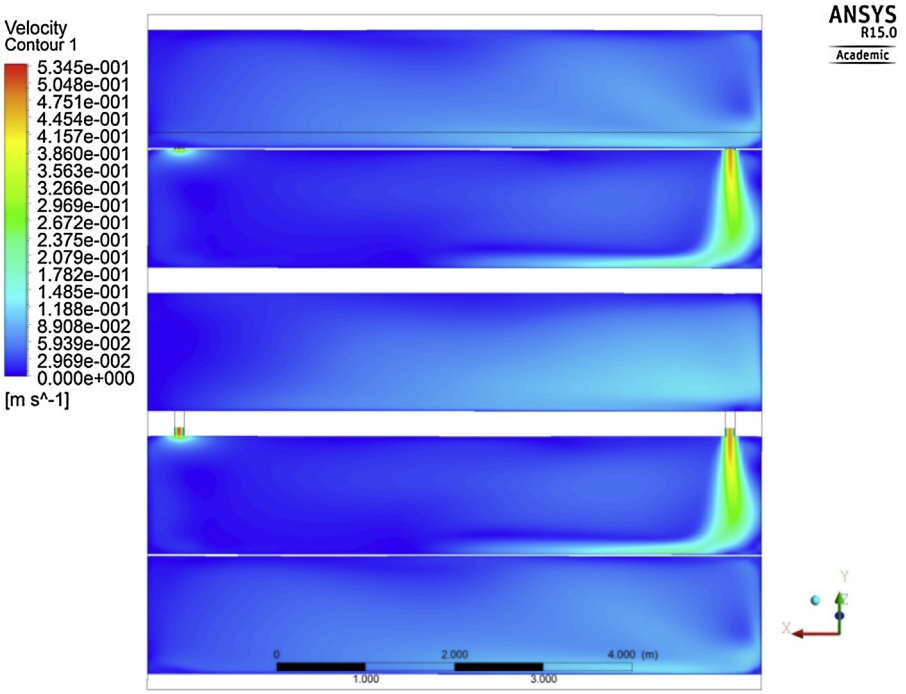

Fig. 5. Contours of velocity magnitude of air stream inside the classroom.

flow velocity in the inlet section was equal to 0.463 m s^{-1} which contributed to an air exchange rate of 3.3 h^{-1}.

According to Fig. 5, the highest flow velocities, ranging between 0.1 and 0.3 m s^{-1}, were observed in the two zones corresponding to the inlet flow sections. Consequently, the more exposed building materials to the convective air flow were the side walls and mainly the flooring near the inlet sections. Average velocity inside the room was 0.036 m.s^{-1}. Furthermore, the mean air flow velocity inside the room (U_m), calculated from Eq. (7) was equal to 6.55×10^{-3} m s^{-1}, which underestimated the flow velocity particularly in the inlet sections and consequently the convective mass transfer coefficient h_{ij} calculated from Eq. (6) is 1.4×10^{-4} m s^{-1}. Another assumption of the box model was to consider the room as a well-mixed reactor, which implies generally a turbulent flow to obtain a homogeneous concentration of pollutant. However, the fluid flow in indoor environment was generally laminar. Here, the highest Reynolds number of the room was in the inlet section and was equal to 6348 (the limit value between laminar and transition flow was near 5×10^5). Another key parameter in the homogeneity of pollutant concentration was the mechanism of transport of the pollutant in the gas phase which was governed by the convection–diffusion equation [39]. In indoor environment, the diffusive transport of pollutant should also be considered due to low flow velocity of air and could become the main process of pollutant transport. It could be simply formulated as follows: a low air flow velocity led generally to high mean residence time of air in the room which induced high mean diffusion time, favorable to the homogenization of the pollutant concentration in indoor air. The well-mixed state was generally obtained with a turbulent flow associated to a convective transport. Consequently, the high value of air exchange rate in the studied case (3.3 h^{-1}) induced a relative low mean residence time (18 min), which may be favorable to a convective transport. This point was discussed by CFD simulation of formaldehyde transport in the indoor air of the classroom.

Table 4
CFD simulation main results and comparison with box model.

Zone	CH_2O mean concentration (μg m^{-3})	Mean velocity (m s^{-1})
Floor	20.00	0.000
Plane aligned with floor at		
z = 0.01 m	14.85	0.040
z = 0.02 m	13.01	0.055
z = 0.03 m	12.27	0.060
z = 0.04 m	11.60	0.064
z = 0.05 m	11.40	0.060
z = 0.06 m	11.08	0.062
z = 0.1 m	10.65	0.064
z = 0.15 m	10.25	0.061
Outlets	9.26	0.463
Room volume	9.30	0.036
Room volume box model	5.8	6.55×10^{-3}

Model	Floor emission rate τ (μg m^{-2} s^{-1})	Mass transfert coefficient h_{ij} (m s^{-1})
CFD model	1.05×10^{-2}	9.8×10^{-4}
Box model	1.93×10^{-3}	1.4×10^{-4}

4.2. Study of the distribution of the formaldehyde concentration in indoor air by CFD simulation

To simulate a simple case, only the flooring and the two inlets were considered as formaldehyde sources. The floor was identified as the main source of formaldehyde due to its high surface (49 m^2).

The simulation was carried out in steady-state condition with a constant flooring surface concentration of formaldehyde (20 μg m^{-3} at 292 K or 1.63×10^{-8} in mass fraction) and a constant concentration of formaldehyde in the two inlets (5.0 μg m^{-3} at 292 K or 4.08×10^{-9} in mass fraction). The diffusive transport was modeled with the Maxwell–Stefan's equation [40]. Simulation results were presented in Figs. 6 and 7 and Table 4. The analysis of Fig. 6 highlighted the homogeneity of formaldehyde concentration inside the room, justifying the assumption of well-mixed room. This observation is confirmed by the similar values of mean concentration (9.26 and 9.3 μmol m^{-3}) in the outlets and inside the room, presented in Table 4. This is probably due to the high value of applied air exchange rate (3.3 h^{-1}). However, a concentration

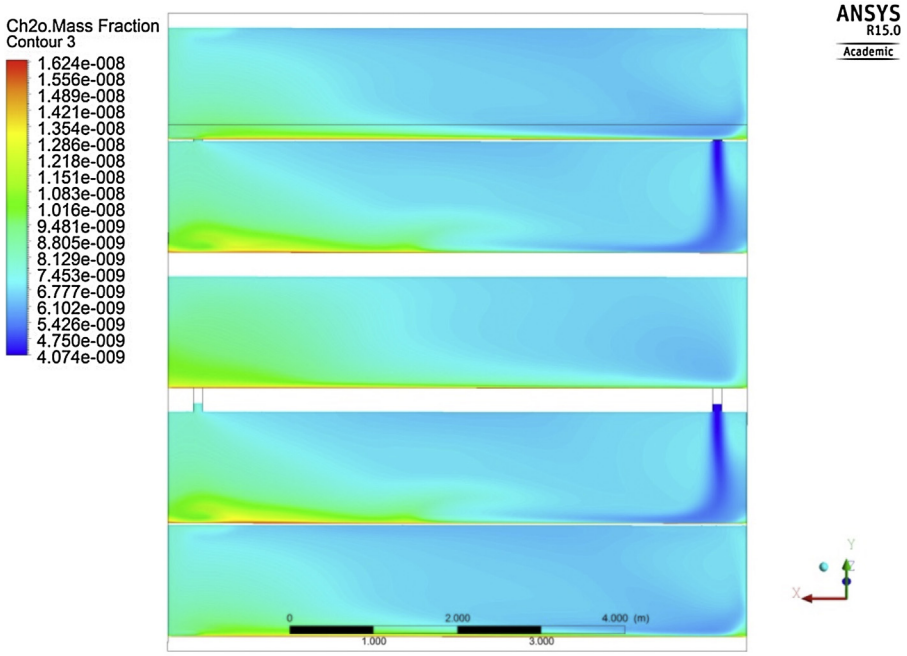

Fig. 6. Profiles of formaldehyde concentration inside the classroom (emission source: floor).

gradient was observed near the floor surface surrounding the outlets due to higher local residence time of air.

The box model was used to calculate the mean convective mass transfer coefficient through the floor boundary layer (h_{ij}) from CFD results (Table 4). The obtained value ($9.8 \times 10^{-4}\,\mathrm{m\,s^{-1}}$) was quite different from that of box model ($1.4 \times 10^{-4}\,\mathrm{m\,s^{-1}}$). The box model underestimated the floor emission contribution compared with the CFD approach. This fact could be explained by the direction and the flow rate of the inlet air stream, normal to the floor surface, reducing the boundary layer and increasing the convective transfer near the zones surrounding the inlet sections (Fig. 7). The formaldehyde concentration in a plane aligned with floor surface at a distance of 0.02 m was similar to that of inlet air stream in the area surrounding the inlet zones and consequently the local boundary layer is less than 0.02 m. This could explain the higher convective mass transfer coefficent of the CFD model than the box model.

The outlet concentrations of CFD and box model were 9.3 and $5.8\,\mu\mathrm{g\,m^{-3}}$ respectively, showing the main effect of the air exchange on the indoor air concentration. In summary, the box model underestimated the indoor concentration, compared with the CFD model.

As shown in this figure, the level of formaldehyde in indoor air was not exceeding to 7.0×10^{-9} in mass fraction (or $8.6\,\mu\mathrm{g\,m^{-3}}$). This low concentration magnitude showed that the indoor

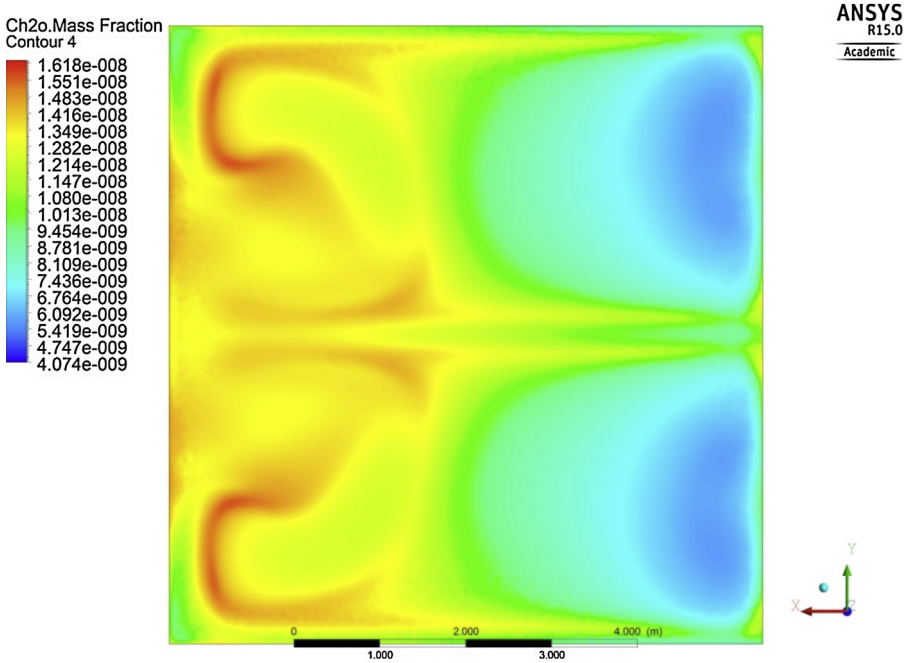

Fig. 7. Profiles of formaldehyde concentration on a plane aligned with floor surface at a distance $z = 0.02$ m.

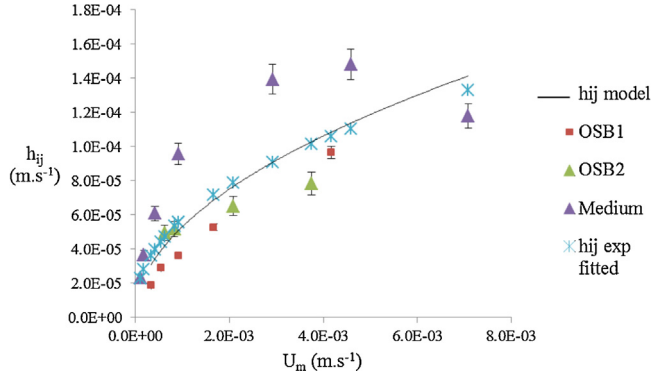

Fig. 8. Comparison between experimental and theoretical convective mass transfer coefficient of formaldehyde (h_{ij}) versus mean flow velocity (U_m).

concentration was mainly influenced by the convective transport of formaldehyde from inlet flow, due to the high value of applied air exchange rate (3.3 h^{-1}). Moreover, this study highlighted the minor contribution of flooring to indoor pollution. Indeed, the diffusive transport was observed mainly in the areas surrounding the outlets due to high local residence time of air favorable to the diffusive mass transfer from flooring surface to indoor air. This simulation showed that the assumption of well-mixed room was a simplified approach of the real material/air mass transfer process even if this indoor area was fairly homogeneous. The box model was then applied to this simulate case to comparing the results.

The mean air velocity inside the room (U_m) was equal to 6.55×10^{-3} m s^{-1}, as discussed previously. The characteristic length of the material/fluid system (L_c) was equal to the ceiling height (2.7 m). The value of formaldehyde air diffusion coefficient (D_{iair}) was estimated by Fuller, Schettler and Giddings (FSG) method (1.66×10^{-5} m^2 s^{-1} at 292 K). Then, the value of the theoretical convective mass transfer (h_{ij}) calculated from Eq.(6) was estimated to be 1.36×10^{-4} m s^{-1}. The mean concentration of formaldehyde calculated from Eq. (8) was equal to 5.77 μmol m^{-3} (4.7×10^{-9} in mass fraction). The CFD simulated mean concentration in indoor air was equal to 7.0 μmol m^{-3} (5.7×10^{-9} in mass fraction). This result showed that the simple box model permits a good estimation of the indoor quality. This could be explain by the main effect of convective transport leading to high impact of outdoor concentration on mean indoor concentration whereas the contribution of the flooring was low.

For the box model, the contribution of building materials to indoor air pollution was estimated by the quantification of the convective mass transfer coefficient (h_{ij}), discussed in the next section.

4.3. Study of experimental and theoretical determination of the convective mass transfer coefficient of formaldehyde h_{ij}

The experimental determination of the convective mass transfer (h_{ij}) was performed using the CLIMPAQ 50 L test chamber, as detailed in the Material and methods section. The main results of this study were summarized in Fig. 8. Results showed a significant difference between the values of the experimental coefficients of the MDF and the two OSB materials. This observation suggested that the nature of the material or/and its surface properties had an influence on the mass transfer process. From a theoretical point of view, the convective mass transfer of formaldehyde in laminar flow was governed by the molecular diffusion through the boundary layer on the material surface [41]. Hence, the material surface itself should not affect the mass transfer through the boundary layer.

The solid line curve in Fig. 8 showed the theoretical value of h_{ij}, calculated from Eq.6, as versus of the mean flow velocity (U_m). Its equation was:

$$h_{ij} = 1.68 \times 10^{-3} \times U_m^{0.5} \quad \text{with} \quad r^2 = 1.0 \tag{17}$$

A fitting curve to experimental data of the three materials was also represented. Its equation was:

$$h_{ij} = 1.1 \times 10^{-3} \times U_m^{0.4269} \quad \text{with} \quad r^2 = 0.69 \tag{18}$$

Despite the dispersion of some experimental points (MDF material), the fitting and the theoretical curves (Eq. (6)) were almost superimposed, showing the high degree of convergence of the two approaches. This preliminary result was significant with the purpose of quantitative validation of the convective mass transfer coefficient value. However, other materials should be tested to consolidate this observation.

The knowledge of both on-site gas phase concentration at material surface and convective mass transfer coefficient allowed us to study the impact of building materials on indoor air pollution using a box model, detailed in the Theoretical basis section.

4.4. Study of the impact of building materials on indoor air pollution

During each measurement campaign, formaldehyde surface concentration was determined for the twelve materials described in Table 2. Measurements of gas phase concentrations at material surfaces (C_{sij}), indoor (C_i) and outdoor (C_{iout}) air concentrations during 5 weeks were summarized in Table 5. Formaldehyde concentration at material surface changed a lot from one week to another, showing the interest of on-site measurement. The presence of new materials could explain this evolution with time. Indeed, formaldehyde emissions usually tend to stabilize with time. Transfer of formaldehyde could occur on the surfaces of various materials by adsorption/desorption with possible chemical reactions. Moreover, formaldehyde emissions released from materials are also known to be variable depending on the temperature and humidity. Desks were found to be the materials emitting the highest quantity of formaldehyde which was no surprising as they were made with particle boards. Upper (6) and under (7) side of the desks did not have the same surface concentration, respectively 23 and 85 μg m^{-3} in week 4, as coatings were different. The formaldehyde diffusion from the particle board to the surface was then different depending on the sides. Interactive board (2) also presented a relative high surface concentration (from 36 to 116 μg m^{-3}); this was certainly due to a melamine resin (containing formaldehyde) which covers the screen. The box model was applied to these data (Table 5). Uncertainties of the modeled concentrations were calculated from Eqs. (9)–(13). Results show a good agreement between measured and calculated formaldehyde concentrations despite a relatively high standard deviation.

The low difference between the indoor and outdoor air concentrations (from 0 to 7.7 μg m^{-3}) highlighted the impact of outdoor air via the ventilation on indoor air concentration. This fact could be explained by the high value of air exchange rate (3.3 h^{-1}) and the associated convective effect predominant in the transport of formaldehyde in this indoor environment. This result was in agreement with the previous results of CFD modeling.

Building materials and outdoor air (via ventilation) contributions to indoor air formaldehyde levels will be now discussed from data in Table 6. Globally, the materials contribution was low (from −7 to 41%) compared to outdoor air (from 59 to 107%), due to the high air exchange rate. A negative contribution (−7%) was observed on week 3 meaning that materials played a role of sink for formaldehyde and act as air cleaners. This was supported by the difference

Table 5
Comparison between measured and modeled formaldehyde average concentration in the classroom for five weeks (LOD = 0.005 μg m^{-3}).

Week no.	1	2	3	4	5
Material (no.)			C_{sij} (μg m^{-3})		
1	5.6 ± 0.9	10.2 ± 1.6	0.8 ± 0.1	13.7 ± 2.2	27 ± 4
2	63 ± 10	36 ± 6	54 ± 9	85 ± 14	116 ± 18
3	13.3 ± 2.1	8.3 ± 1.3	7.9 ± 1.3	24 ± 4	50 ± 8
4	< LOD	8.3 ± 1.3	2.2 ± 0.3	10.2 ± 1.6	4.6 ± 0.7
5	< LOD	6.9 ± 1.1	12.9 ± 2.1	5.5 ± 0.9	<LOD
6	28 ± 5	15.9 ± 2.5	8.1 ± 1.3	23 ± 4	49 ± 8
7	49 ± 8	34 ± 5	43 ± 7	85 ± 14	116 ± 18
8	< LOD	8.7 ± 1.4	1.2 ± 0.2	6.0 ± 1.0	6.9 ± 1.1
9	0.6 ± 0.1	9.0 ± 1.3	12.9 ± 2.1	13.3 ± 2.1	6.1 ± 1.0
10	5.4 ± 0.9	10.8 ± 1.4	6.3 ± 1.0	12.8 ± 2.0	36 ± 6
11	6.5 ± 1.0	14.9 ± 2.4	8.3 ± 1.3	8.3 ± 1.3	53 ± 9
12	62 ± 10	24 ± 4	33 ± 5	151 ± 24	87 ± 14
C_{iout}	5.2 ± 2.3	5.0 ± 2.3	12.9 ± 2.3	6.0 ± 2.3	6.0 ± 2.3
Measured C_i	5.6 ± 2.3	5.6 ± 2.3	12.9 ± 2.3	13.7 ± 2.3	13.5 ± 2.3
Modeled C_i	5.9 ± 4.6	5.9 ± 4.6	12.1 ± 4.4	8.3 ± 4.8	10.2 ± 5.1

between the outdoor concentration (12.9 μg m^{-3}) and the flooring surface concentration (7.9 μg m^{-3}).

The suspended ceiling (4) and the painted walls (8) were also alternatively sources and sinks of formaldehyde. This shows that the mass transfer at the material/air interface was a reversible process governed by an adsorption/desorption equilibrium. This behavior was also observed with the curtain (10), only made of polyester and thus containing no formaldehyde itself. This effect could be accentuated by the high surface area developed by their fibrous texture. This result highlighted that even formaldehyde free materials could become emitters regarding the interactions with other emissive materials and the conditions of use of the building.

Regarding the box model, the low materials contribution to indoor air formaldehyde could explain the good agreement between measured and calculated formaldehyde concentration. The model performance should be further consolidated from experimental case studies presenting low air exchange rates and high emissive building materials.

This study highlights the temporal variability of the behavior of some building materials which act as formaldehyde sources or sinks in indoor environment. An improvement ot the modeling approach could be both to collect on-site measurements to define real material/air mass transfer processes and to implement a box model integrating adsorption/desorption processes, based on the work of Elkilani [29]. Further advantage of this approach lies in the ability to quite easily implement chemical reactions in such model.

Table 6
Building materials and outdoor air (via ventilation) contributions to indoor air formaldehyde concentration in the studied classroom.

Week no.	1	2	3	4	5
Material (no.)	Material contribution $Q_{ij}/\lambda C_i \times 100$ (%)				
1	−0.02	0.18	−0.24	0.17	0.43
2	2.00	1.04	0.73	1.95	2.18
3	6.69	2.10	−1.88	10.47	21.11
4	−3.21	1.24	−2.63	0.75	−1.76
5	−0.74	0.11	0.05	−0.25	−0.74
6	4.14	1.83	−0.36	1.96	4.25
7	8.74	5.66	3.16	11.30	12.64
8	−5.78	2.62	−5.21	−1.58	−1.87
9	−0.07	0.04	0.01	0.05	−0.03
10	−0.11	0.98	−0.58	0.67	3.10
11	0.02	0.33	−0.07	0.00	0.94
12	1.04	0.34	0.20	1.92	0.83
$\sum Q_{ij}/\lambda C_i$	12.70	16.48	−6.83	27.40	41.09
	Outdoor air contribution via ventilation $C_{iout}/C_i \times 100$				
C_{iout}/C_i	87.30	83.52	106.83	72.60	58.91
Total	100	100	100	100	100

5. Conclusion

Formaldehyde emission behavior of building materials in a newly built classroom was investigated by on-site measurements of surface concentration and quantification of the convective mass transfer through the boundary layer at material surface. An experimental method to estimate this parameter from measurements of both surface concentration and emission rate of materials in an emission test chamber was developed. An empirical relationship between this parameter and the mean flow velocity (U_m) was proposed to quantify the contribution of building materials to indoor air pollution versus ventilation conditions.

On-site measurements of gas phase concentration at material surface brought out that adsorption/desorption phenomena could occur. This induces a temporal variability of the behavior of some building materials, acting as formaldehyde sources or sinks according to the conditions of use of the building. Moreover, even formaldehyde free materials (for example here, the polyester curtains) could become potential emitters after significant adsorption of formaldehyde. These results show the interest of on-site measurements of material surface concentration to investigate the material/indoor air mass transfer and to predict the indoor air pollution.

Given these first results, the box model seems to be a practical and an easy-use tool to estimate the indoor air quality in high ventilated environments similar to the studied classroom. This fact could be explained by the high contribution of outdoor air to indoor air pollution level in this context.

References

[1] N.E. Klepeis, W.C. Nelson, W.R. Ott, J.P. Robinson, A.M. Tsang, P. Switzer, J.V. Behar, W.H. Engelmann, The National Human Activity Pattern Survey (NHAPS): a resource for assessing exposure to environmental pollutants, J. Expos. Anal. Environ. Epidem. 11 (2001) 231–252.

[2] T. Alsmo, S. Holmberg, Sick buildings or not: indoor air quality and health problems in schools, Indoor Built Environ. 16 (2007) 548–555.

[3] M. Chai, J. Pawliszyn, Analysis of environmental air samples by solid-phase microextraction and gas chromatography/ion trap mass spectrometry, Environ. Sci. Technol. 29 (1995) 693–701.

[4] ECA, Indoor Air Quality & Its Impact on Man, Report 18, Evaluation of VOC Emissions from Building Materials, Office for Official Publications of the European Communities, 1997.

[5] AgBB, Ausschuss zur gesundheitlichen Bewertung von Bauprodukten, Health-related Evaluation Procedure for Volatile Organic Compounds Emissions (VOC and SVOC) from Building Product, 2008.

[6] AFSSET, Agence Française de Sécurité Sanitaire de l'Environnement et du Travail, Procédure de Qualification des Produits de Construction et de Décoration sur la Base de Leurs Émissions de COV et de Formaldéhyde et de Critères Sanitaires, Rapport du Groupe de Travail Afsset «COV et Produits de Construction», Saisine 2004/011, Paris, 2009.

[7] J.Y. An, S. Kim, H.J. Kim, T.V.O.C. Formaldehyde, emission behavior of laminate flooring by structure of laminate flooring and heating condition, J. Hazard. Mater. 187 (2011) 44–51.
[8] M. Bohm, M.Z.M. Salemb, J. Srbaa, Formaldehyde emission monitoring from a variety of solid wood, plywood, blockboard and flooring products manufactured for building and furnishing materials, J. Hazard. Mater 221–222 (2012) 68–79.
[9] ISO 16000-9, Indoor Air, Part 9: Determination of the Emission of Volatile Organic Compounds from Building Products and Furnishing-Emission Test Chamber Method, 2006.
[10] ISO 16000-10, Indoor Air, Part 10: Determination of the Emission of Volatile Organic Compounds from Building Products and Furnishing-Emission Test Cell Method, 2006.
[11] N. Shinohara, M. Fujii, A. Yamasaki, Y. Yanagisawa, Passive flux sampler for measurement of formaldehyde emission rates, Atmos. Environ. 41 (2007) 4018–4028.
[12] N. Shinohara, Y. Kai, A. Mizukoshi, M. Fujii, K. Kumagai, Y. Okuizumi, M. Jona, Y. Yanagisawa, On-site passive flux sampler measurement of emission rates of carbonyls and VOCs from multiple indoor sources, Build. Environ. 44 (2009) 859–863.
[13] A. Blondel, H. Plaisance, Validation of a passive flux sampler for on-site measurement of formaldehyde emission rates from building and furnishing materials, Anal. Meth. 2 (2010) 2032–2038.
[14] S. Yamashita, K. Kume, T. Horiike, N. Honma, M. Fusaya, T. Ohura, T. Amagai, A simple method for screening emission sources of carbonyl compounds in indoor air, J. Hazard. Mater. 178 (2010) 370–376.
[15] J. Nicolle, V. Desauziers, P. Mocho, Solid phase microextraction sampling for a rapid and simple on-site evaluation of volatile organic compounds emitted from building materials, J. Chromatogr. A 1208 (2008) 10–15.
[16] J. Nicolle, V. Desauziers, P. Mocho, O. Ramalho, Optimization of FLEC®-SPME for field passive sampling of VOCs emitted from solid building materials, Talanta 80 (2009) 730–737.
[17] P. Mocho, V. Desauziers, Static SPME sampling of VOCs emitted from indoor building materials: Prediction of calibration curves of single compounds for two different emission cells, Anal. Bioanal. Chem. 400 (2011) 859–870.
[18] C. Garden, S. Semple, K. De Brouare, INTERA B4 Project, A Review of Existing Indoor Pollutant Exposure Data and Models, Integrated Exposure for Risk Assessment in Indoor Environments (INTERA), 2011.
[19] National Research Council, Indoor Pollutants, National Academy Press, Washington, 1981.
[20] W.W. Nazaroff, G.R. Cass, Mathematical modelling of chemically reactive pollutants in indoor air, Environ. Sci. Technol. 20 (1986) 924–934.
[21] P.B. Ryan, J.D. Spengler, P.F. Halfpenny, Sequential box models for indoor air quality: application to airliner cabin air quality, Atmos. Environ. 22 (1987) 1031–1038.
[22] Z. Ren, J. Stewart, Prediction of personal exposure to contaminant sources in industrial buildings using a sub-zonal model, Environ. Modell. Softw. 20 (2005) 623–638.
[23] B. Deng, C.N. Kim, CFD simulation of VOCs concentrations in a resident building with new carpet under different ventilation strategies, Build. Environ. 42 (2007) 297–303.
[24] R. Ramponi, B. Blocken, CFD simulation of cross-ventilation for a generic isolated building: Impact of computational parameters, Build. Environ. 53 (12) (2012) 34–48.
[25] R. Atkinson, D.L. Baulch, R.A. Cox, J.N. Crowley, R.F. Hampson, R.G. Hynes, M.E. Jenkin, M.J. Rossi, J. Troe, Evaluated kinetic and photochemical data for atmospheric chemistry: Volume II – gas phase reactions of organic species, Atmos. Chem. Phys. 6 (2006) 3625–4055.
[26] M.E. Jenkin, S.M. Saunders, M.J. Pilling, The tropospheric degradation of volatile organic compounds: a protocol for mechanism development, Atmos. Environ. 31 (1997) 81–104.
[27] N. Carslaw, A new detailed chemical model for indoor air pollution, Atmos. Environ. 41 (2007) 1164–1179.
[28] R. Kamens, M. Jang, C.-J. Chien, K. Leach, Aerosol formation from the reaction of α-pinene and ozone using a gas- phase kinetics-aerosol partitioning model, Environ. Sci. Technol. 33 (1999) 1430–1438.
[29] A. Elkilani, W. Bouhamra, B.D. Crittenden, An indoor air quality model that includes the sorption of VOCs on fabrics, Process Saf. Environ. Protec. 79 (2001) 233–243.
[30] F.M. White, Heat and Mass Transfer, Addison-Wesley, Reading, Massachusetts, 1988.
[31] C.R. Reid, J.M. Prausnitz, B.E. Poling, The Properties of Gases and Liquids, McGraw Hill Inc., New York, 1987.
[32] V. Desauziers, B. Auguin, Device and method for gas sampling, French Patent Pending no. 1003271, 21012.
[33] V. Desauziers, B. Auguin, SPME-adapter: a rapid sampling for the analysis of VOCs traces in air. Techniques de l'Ingénieur, IN 149, TI Editions, 2012.
[34] V. Larroque, V. Desauziers, P. Mocho, Study of preservation of polydimethylsiloxane/carboxen solid-phase microextraction fibres before and after sampling of volatile organic compounds in indoor air, J. Chromatogr. A 1124 (2006) 106–111.
[35] J.A. Koziel, J. Noah, J. Pawliszyn, Field sampling and determination of formaldehyde in indoor air with solid-phase microextraction and on-fiber derivatization, Environ. Sci. Technol. 35 (2001) 1481–1486.
[36] V. Desauziers, Traceability of pollutant measurements for ambient air monitoring, Trends Anal. Chem. 23 (2004) 252–260.
[37] J.A. Koziel, P.A. Martos, J. Pawliszyn, System for the generation of standard gas mixtures of volatile and semi-volatile organic compounds for calibrations of solid-phase microextraction and other sampling devices, J. Chromatogr. A 1025 (2004) 3–9.
[38] ASTM, E 741-00, Standard Test Method for Determining Air Change in a Single Zone by Means of Tracer Gas Dilution, 2006.
[39] H.G. Roos, M. Stynes, L. Tobiska, Numerical Methods for Singularly Perturbed Differential Equations: Convection-Diffusion and Flow Problems, Springer, 1996.
[40] E.L. Cussler, Diffusion Mass Transfer in Fluid Systems, Cambridge University Press, 1997.
[41] R.E. Treybal, Mass Transfer Operations, McGraw Hill Inc. (1981).